Brain Research Bulletin, Vol. 51, No. 5, pp. 393–399, 2000

0361-9230/00/$–see front matter

PII S0361-9230(99)00256-7

A reduced compartmental model of the mitral cell for use in network models of the olfactory bulb

Andrew P. Davison,* Jianfeng Feng and David Brown

Laboratory of Computational Neuroscience, The Babraham Institute, Babraham, Cambridge, UK

[Received 6 August 1999; Revised 3 November 1999]

ABSTRACT: We have developed two-, three- and four-compartment models of a mammalian olfactory bulb mitral cell as a reduction of a complex 286-compartment model [1]. A minimum of three compartments, representing soma, secondary (basal) dendrites and the glomerular tuft of the primary dendrite, is required to adequately reproduce the behaviour of the full model over a broad range of firing rates. Adding a fourth compartment to represent the shaft of the primary dendrite gives a substantial improvement. The reduced models exhibit behaviours in common with the full model which were not used in fitting the model parameters. The reduced models run 75 or more times faster than the full model, making their use in large, realistic network models of the olfactory bulb practical. © 2000 Elsevier Science Inc.

KEY WORDS: Olfaction, Single-neuron models, Simplified models, Biological neural networks.

INTRODUCTION

Just as there are (at least) two levels of enquiry in experimental neuroscience—the cellular and sub-cellular level, investigating synaptic transmission, ion channel function and intra-cellular signalling, and the systems level, recording individual and ensemble neuronal responses and attempting to relate these to behaviour—so there are two levels in computational neuroscience [8], the first exemplified by the classic Hodgkin-Huxley model of ion channel function [7] and by the compartmental/cable modelling of dendrites initiated by Rall (e.g., [13]), the second taking extremely simplified single neurone models but connecting them in large networks.

In modelling there is great potential for bridging the gap between these two levels of enquiry, which can mutually constrain and inform one another, using networks of neurones with a level of complexity and biological fidelity intermediate between highly detailed multi-compartmental models and simple network models. A number of strategies have been used to construct such intermediate-complexity single cell models. All take as their starting point a detailed compartmental neurone model and attempt to simplify it while retaining the electrotonic properties and/or input-output behaviour of the detailed model. One strategy is to concentrate on the electrotonic properties and reduce the number of compartments in the cell while conserving the membrane time constants and the cell input resistance [3,15]. A more drastic strategy is to attempt to abstract the key features of the cell into as few compartments and channel types as possible, and constrain the simplified model to have the same input-output properties as the detailed model, in terms of firing rate response to synaptic or electrical stimulation [11]. Both strategies give both shorter simulation times and potentially greater understanding than the fully-detailed models.

In this paper, we have used the second strategy mentioned above to construct simplified models of olfactory bulb mitral cells. The models are based on a detailed, 286-compartment model published by Bhalla and Bower [1], which was itself based on intra-cellular recordings and detailed morphological measurements. We have found that at least three compartments are necessary for an adequate model of an olfactory mitral cell, with at least one compartment for each of the soma, secondary (basal) dendrites and glomerular tuft. Four compartments gives a substantial improvement on three, with little increase in processing time. The reduced models give a good fit to the full model over a wide range of firing rates. The reduced models have the potential to be a useful tool in realistic network modelling of the olfactory bulb.

MATERIALS AND METHODS

Bhalla and Bower's mitral cell model was re-implemented in the neural simulator *Neuron* and tested against their *Genesis* implementation. The two implementations gave qualitatively the same results but had small quantitative differences (of a few percent in firing rates) which were pinpointed as being due to alternative numerical strategies, mainly the use of symmetric compartments by *Neuron* and asymmetric compartments by *Genesis*.

The results presented by Bhalla and Bower are for stimulating electrodes in the soma. This provides a fairly weak constraint on the model—as Bhalla and Bower noted, some parameters can be varied by an order of magnitude with minimal effect on the output. Since all or almost all of the excitatory input received by mitral cells is to the glomerular dendritic tuft, we first briefly examined the response of their model to glomerular input. When depolarising current is injected into the soma of Bhalla and Bower's mitral cell model, the cell responds with regular firing. With current injected into the glomerular compartments Bhalla and Bower's model produces a double spike at the soma then settles down to regular firing (Fig. 1A). This double spike is produced by a large, extended calcium spike in the glomerulus (Fig. 1B). Is such behaviour observed experimentally? In about half of recorded rat mitral cells,

* Address for correspondence: Andrew P. Davison, Laboratory of Computational Neuroscience, The Babraham Institute, Babraham, Cambridge CB2 4AT, UK. Fax:+44-1223-496031; E-mail: andrew.davison@bbsrc.ac.uk

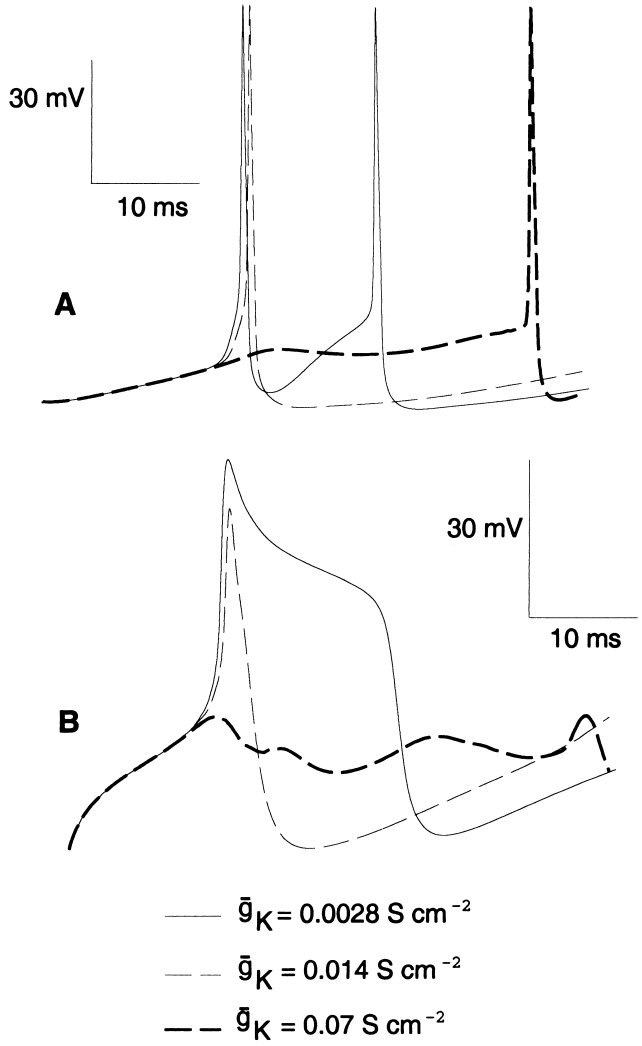

FIG. 1. Response of the full model to a total constant current of 0.4 nA to the glomerulus, divided evenly among the compartments ($\sim$ 4.3 pA per compartment). (A) Somatic membrane potential trace and (B) Membrane potential trace at base of glomerular tuft, for varying $\bar{g}_K$ in the tuft. These figures show the double somatic spike and extended dendritic calcium spike seen with low $\bar{g}_K$, that are removed by increasing the value of the parameter. Increasing $\bar{g}_K$further delays the somatic spike and abolishes the dendritic calcium spike.

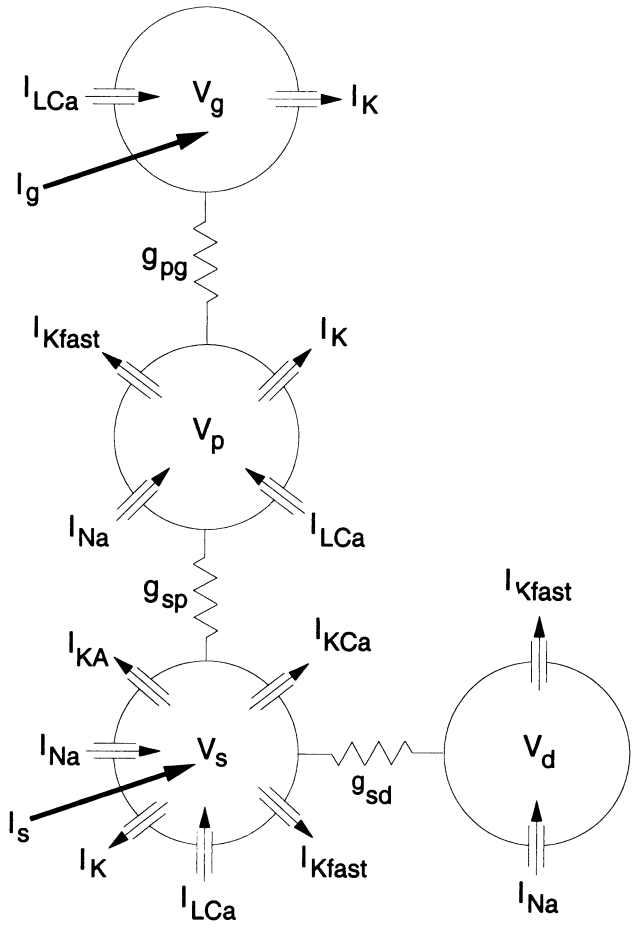

FIG. 2. Schematic of the four-compartment model showing ion channels and points of stimulation. Currents are sodium (I_{Na}), slow potassium delayed rectifier (I_K), fast potassium delayed rectifier (I_{Kfast}), potassium anomalous rectifier (I_{KA}), calcium-dependent potassium (I_{KCa}) and L-type calcium (I_{LCa}). The conductances between soma and secondary dendrite, soma and primary dendrite, and primary dendrite and glomerulus are g_{sd}, g_{sp} and g_{pg}, respectively.

Chen and Shepherd [5] observed fast pre-potentials in response to olfactory nerve stimulation, indicative of dendritic excitability, but these are small amplitude events, not full action potentials. Chen, Midtgaard and Shepherd [4] recorded from the primary dendrite just proximal to the glomerular tuft as well as from the soma, and on some occasions observed an action potential in the dendrite preceding that in the soma. These were of similar width to the somatic action potentials, not the extended depolarisation seen in the Bhalla-Bower model. Apparent double spikes have been observed when the cell is already depolarised (see Fig. 6A of [10]), but these appear to be rare occurrences. Therefore, we conclude that the glomerular tuft in Bhalla and Bower's model, as it stands, is over-excitable.

A simple parameter change was found to eliminate the double spiking—increasing the density of K channels in the glomerular compartments by a factor of five produces only a short calcium spike which gives rise to a single spike at the soma (Fig. 1). Increasing the K channel density by a further factor of five eliminates the glomerular/dendritic calcium spike and increases the latency of the somatic spike. These changes in K channel density have no visible effect on the model response to somatic current injection (data not shown).

For fitting of the reduced models we used a K channel density in the glomerular compartment of $\bar{g}_K = 0.02$ S cm^{-2}, about seven times larger than that used by Bhalla and Bower. All other parameter values were as published by them.

To simplify the model we used the same strategy as Pinsky and Rinzel [11] in their simplification of Traub's [16] hippocampal pyramidal neurone model—namely to retain the same active currents and gating kinetics, with the same channel densities/maximum conductances, but to drastically reduce the number of compartments. The full Bhalla and Bower model has 286 compartments; we investigated simplifications with two, three or four compartments.

The two-compartment model has one compartment for the

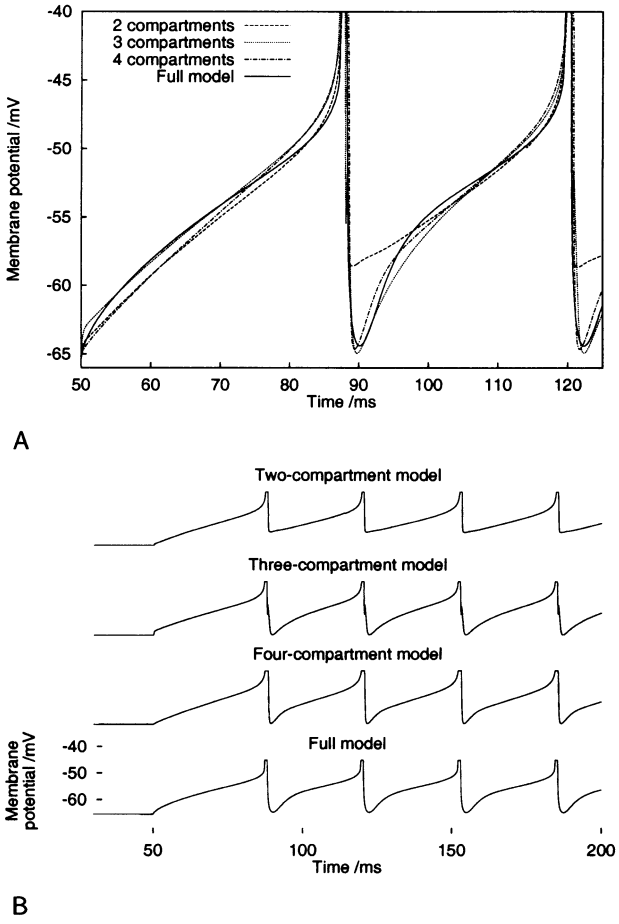

FIG. 3. Somatic membrane potential trace for full and reduced models with $I_{full} = 0.4\ \mu A\ cm^{-2}$ after fitting to spike shape. Both three- and four-compartment models give good fits to the full model. The two-compartment model has a markedly raised reset potential.

soma and one for the primary dendrite tuft in the glomerulus. The three-compartment model adds a compartment for the secondary dendrites. The four-compartment model (Fig. 2 shows a schematic representation) adds a compartment for the primary dendrite shaft between the soma and glomerular tuft. The correspondence of these compartments to the parts of the real neurone is of course only approximate in such a reduced model. Bhalla and Bower used different conductances in the proximal and distal sections of the secondary dendrites. Our secondary dendrite compartment includes only the distal dendrite conductances. The axon is not represented explicitly in our model. It may be considered to be subsumed into the soma compartment.

The current balance equations for the four compartments (soma, glomerulus, primary dendrite, secondary dendrite) are:

$$C_m V_s' = -I_{leak} - I_{Na} - I_{Kfast} - I_K - I_{KA} - I_{KCa} - I_{Ca} + (g_{sd}/p) \times (V_d - V_s) + (g_{sp}/p)(V_p - V_s) + I_s/p$$

$$C_m V_g' = -I_{leak} - I_K - I_{Ca} + (g_{pg}/q)(V_p - V_g) + I_g/q$$

$$C_m V_p' = -I_{leak} - I_{Na} - I_{Kfast} - I_K - I_{Ca} + (g_{sp}/r)(V_s - V_p) + (g_{pg}/r)(V_g - V_p)$$

$$C_m V_d' = -I_{leak} - I_{Na} - I_{Kfast} - (g_{sd}/s)(V_s - V_d)$$

where V_s, V_g, $V_p$and V_d are the membrane potentials of the somatic, glomerular, primary dendritic and secondary dendritic compartments respectively. Currents and conductances are expressed as densities with units of $\mu A\ cm^{-2}$ and $mS\ cm^{-2}$, respectively. Capacitance (C_m) is in units $\mu F\ cm^{-2}$ and time is in units ms. The Hodgkin-Huxley formalism is used for all channels. The gating equations for the channels are exactly as given in Bhalla and Bower [1]. p is the ratio of the surface area of the soma compartment to the total cell membrane area, q, r and s are the ratios of the glomerular, the primary dendrite and the secondary dendrite surface areas respectively to the total surface area ($p + q + r + s = 1$), g_{sd}, g_{sp}, g_{pg} are the conductances joining the soma and secondary dendrite, soma and primary dendrite, and primary dendrite and glomerular compartments respectively. The equations are similar for the two- and three-compartment models, but with g_{sg} instead of g_{sp} and g_{pg}. The stimulating currents, I_s and I_g are given by:

$$I_s = \alpha_s I_{full}$$

$$I_g = \alpha_g I_{full}$$

where I_{full} is the stimulating current applied to the soma or glomerular compartment of the full model, α_s and α_g are constant

TABLE 1

BEST FIT PARAMETER VALUES

Number of compartments	Fit to Spike Shape			Fit to Spike Times		
	2	3	4	2	3	4
p*	0.166	0.0500	0.0475	0.274	0.0845	0.0510
q	–	0.299	0.184	–	0.14	0.0840
r	–	–	0.216	–	–	0.328
g_{sg}	8.39×10^{-4}	4.87×10^{-5}	–	2.09×10^{-3}	4.44×10^{-5}	–
g_{sd}	–	1.85×10^{-4}	3.31×10^{-2}	–	3.13×10^{-4}	1.94×10^{-4}
g_{sp}	–	–	2.33×10^{-4}	–	–	5.47×10^{-5}
g_{pg}	–	–	4.08×10^{-3}	–	–	5.86×10^{-5}
α_s	1.43	1.35	1.44	2.60	1.78	1.37
α_g	–	–	–	3.02	1.84	1.85

* Units of g_{sg}, g_{sd}, g_{sp} and g_{pg} are $S\ cm^{-2}$. Other parameters are dimensionless.

factors. These 'current factors' are intended to adjust for differences in the input resistance of the models. For each run the current inputs were set to zero for the first 50 ms then stepped up to I_s or I_g. A current step was used to stimulate the models to match the current clamp stimulation used by Bhalla and Bower. To test whether a current step is a good approximation to synaptic input in the glomerulus we modelled synaptic input with 940 α-amino-3-hydroxy-5-methyl-4-isoxazolepropionic acid and N-methyl-D-aspartate synapses, with equal maximum conductances (100 pS) receiving input from independent Poisson processes with mean rates from 4 to 200 Hz. We observed an approximately linear relationship between the constant current needed to produce a particular output firing rate and the synaptic input frequency needed to produce the same output rate. Therefore, we concluded that constant current was a reasonable approximation to synaptic input in these cells.

The maximum conductances of the voltage-gated currents and the membrane capacitance are all fixed to the values used in Bhalla and Bower [1]. The numbers of parameters are therefore four, six and eight for the two-, three- and four-compartment models, respectively. It would of course be possible to vary the maximum conductances to obtain a better fit. However, this would add 14 extra parameters for the four-compartment model, hence increasing the difficulty of fitting the model and increasing the possibility of over-fitting. We used the Downhill Simplex algorithm [12] to fit the simplified models to the full model, with two criteria for evaluating goodness of fit. Our preliminary criterion was:

- The squared difference between voltage traces of simplified and full models over the first 200 ms for current injection to the soma of $I_{\text{full}} = 0.4\ \mu\text{A cm}^{-2}$.

This criterion is referred to henceforth as 'fit-to-shape'. It was hoped that fitting to spike shape, rather than simply to firing rate, would capture some of the important features of the full model dynamics, so that fitting at one input level would give a good fit at all levels. This proved not to be the case (see Results), so a second criterion was used which explicitly averages over input levels and over somatic and 'synaptic' input:

- The squared proportional difference in spike time for the first four spikes, summed over current injections of $I_{\text{full}} = 0.2$, 0.4, 0.8, 1.6 μA cm^{-2} to the soma and to the glomerulus, i.e., if t_k^{reduced} and t_k^{full} are the times of the peaks of the kth spikes in the reduced and full models, then

$$error = \sum_{\substack{\text{soma,}\\ \text{glomerulus}}} \sum_{I_{\text{full}}} \sum_{k=1}^{4} \left(\frac{t_k^{\text{reduced}} - t_k^{\text{full}}}{t_k^{\text{full}}} \right)^2$$

This criterion is referred to henceforth as 'fit-to-time'.

These criteria capture both the transient and steady state behaviour of the models, since the models settle down very quickly into regular firing (the difference between the firing rate calculated from the mean of the first three inter-spike intervals (ISIs) and that calculated from the mean of the 50th to the 100th ISIs is 0.8% for 1.0 nA input and 0.2% for 0.1 nA input to the full model). The firing rates plotted in Figs. 5 and 7 were calculated from the first three ISIs. The range of input currents used produces output firing over the range 10–100 Hz.

All models were simulated in *Neuron* Version 4.1. running on a Digital XP1000 workstation under Digital Unix. The *Neuron* scripts for the reduced models may be obtained from http://www.bi.bbsrc.ac.uk/WORLD/biology/neuro/compneur/compneur.html.

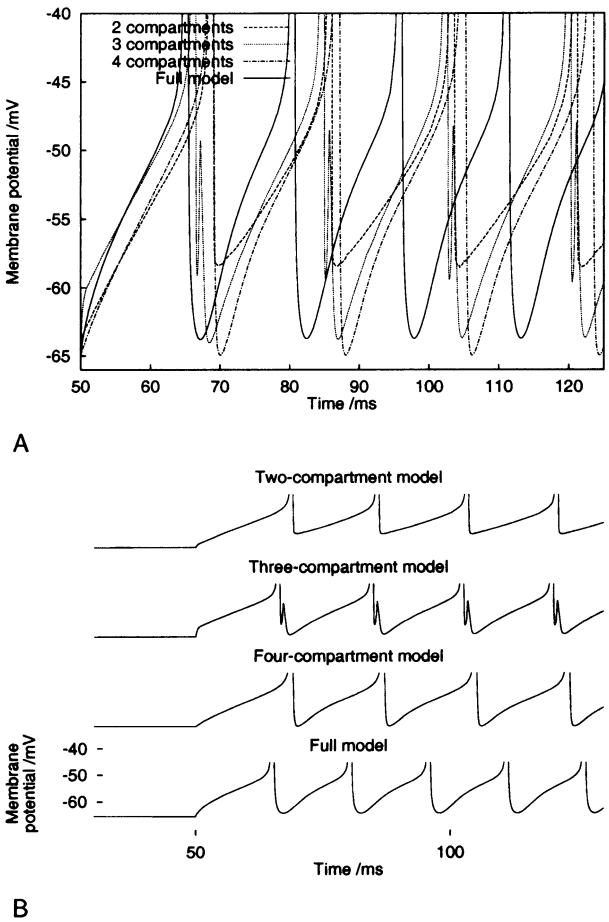

FIG. 4. Somatic membrane potential trace for full and reduced models with $I_{\text{full}} = 0.8\ \mu\text{A cm}^{-2}$ after fitting to spike shape with $I_{\text{full}} = 0.4\ \mu\text{A cm}^{-2}$. The miniature spike on the down-slope of the action potential in the three-compartment model is due to the delay between spiking in the soma and in the secondary dendrite.

RESULTS

Fitting to the Spike Shape

This error measure has several limitations, illustrated by the observation that a simplified model firing with the same frequency as the full model but out of phase with it has a larger error than a model which does not fire at all, although qualitatively it would be regarded as a better match. Nevertheless, using a manual search to obtain a coarse fit and the Simplex optimisation algorithm to refine this, fits were obtained for the two-, three- and four-compartment models. Figure 3 shows the response of the full model and reduced models to current injection of $I_{\text{full}} = 0.4\ \mu\text{A cm}^{-2}$ to the soma. The parameter values are given in Table 1.

The fit is poor for the two-compartment model, with a reset potential of -58 mV compared to -65 mV for the full model (Fig. 3A). The fit is good for the three- and four-compartment models, with the four-compartment model coming closest to reproducing the rapid initial post-spike rebound followed by slower depolarisation exhibited by the full model. The rebound is interpreted as being due to current flow from the calcium channels in the glomerulus to the soma. This is borne out by an experiment in which these channels were removed from the glomerulus of the full

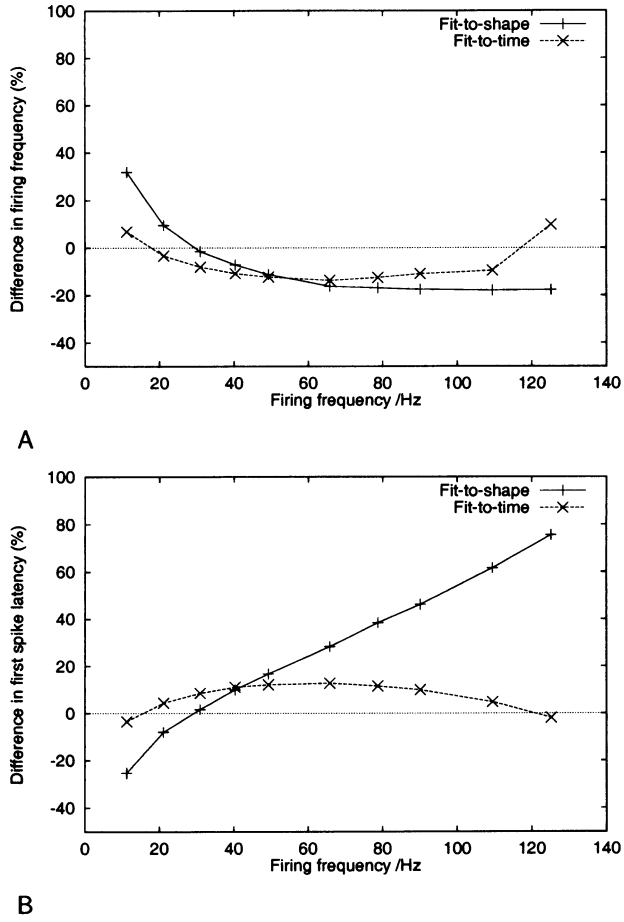

FIG. 5. Comparing fit-to-shape to fit-to-time for the four-compartment model. (A) Firing frequency, (B) latency of first spike. Current was injected in the soma compartment. The four compartment model with fit-to-shape parameters shows almost zero deviation from the full model with current injection 0.4 μA cm^{-2}, the level at which it was fitted, but large differences with higher or lower inputs. In contrast, the four-compartment model with fit-to-time parameters fits reasonably well over a wide range of input levels.

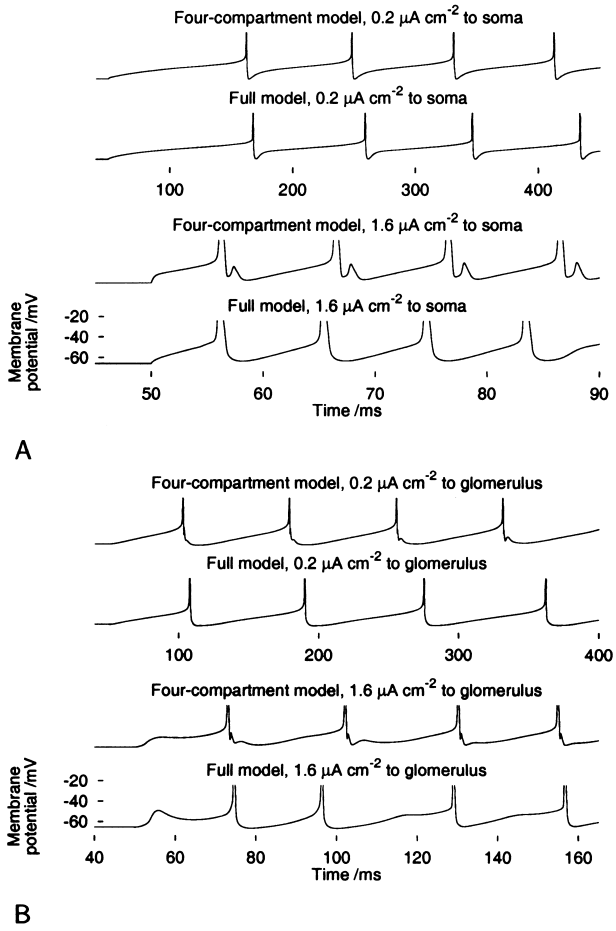

FIG. 6. Somatic membrane potential trace for full and four-compartment models with I_{full} = 0.2 μA cm^{-2} and 1.6 μA cm^{-2} after fitting to spike timing. (A) Current injection to soma. (B) Current injection to glomerulus. The models fit well in terms of first spike latency and firing frequency, but there are discrepancies in the detailed shape of the membrane potential traces. This illustrates one of the problems with very-reduced compartmental models.

model (data not shown). The addition of the primary dendrite compartment in going from three to four compartments is important in delaying the arrival of this current at the soma. The role of the secondary dendrite compartment is chiefly to slow the firing rate. The three-compartment model exhibits a kink in the down-slope of the action potential, which is due to delayed firing in the secondary dendrite.

A good fit under one input condition does not guarantee a good fit under all conditions. Figure 4 shows the discrepancy between the full model and the reduced models with the injected current amplitude doubled. In the three-compartment model, the delay in firing of the secondary dendrite is even more pronounced.

Fitting to Spike Times

The second error measure produces a closer fit in spike timing over a range of input currents (Fig. 5). This is unsurprising since the error measure was designed with this aim in mind. In addition, this error measure is much smoother than the first, and gives greater confidence that the minimum found is close to the global minimum. Fitting to spike shape leads to differences of up to 32% in firing frequency and 76% in the latency of the first spike, for the four-compartment model in the frequency range 10–120 Hz with current injection to the soma. The maximum differences are only 13% and 14% after fitting the same model to spike times. After fitting to spike times the spike shapes of the reduced models are similar to that of the full model but with a deeper hyperpolarisation after the spike and a kink in the down-slope of the action potential, due to delayed firing in the secondary dendrite (Fig. 6).

For somatic current injection, all three reduced models have qualitatively the same behaviour as the full model, but the three- and four-compartment models have a much better quantitative fit to the full model than does the two-compartment model (Figs. 7A,C)

Injecting current into the glomerulus leads to more complex behaviour than somatic injection. Above a certain level, about 1.1 μA cm^{-2} for the full model (giving a firing rate of 40 Hz), the first spike is suppressed by a large slow potassium current in the glomerulus (caused by a large calcium spike) (note the step in first spike latency in Fig. 7D) and the steady-state firing rate is also depressed (Fig. 7B). The three- and four-compartment models also

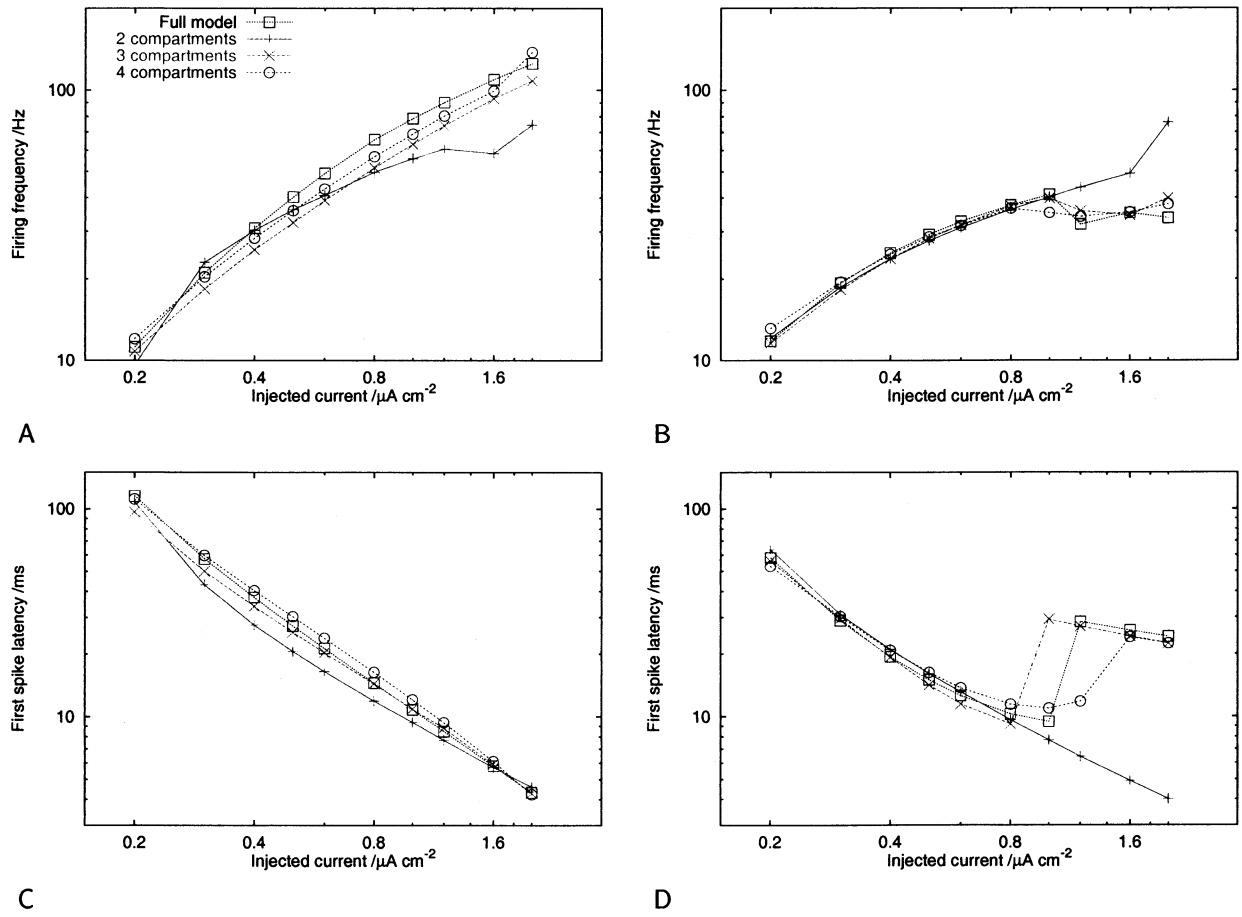

FIG. 7. Comparing reduced models with two, three and four compartments, with fit-to-time parameters: (A) Firing frequency as a function of current for stimulation of soma; (B) as A for stimulation of glomerulus; (C) Latency of first spike as a function of current for stimulation of soma; (D) as C for stimulation of glomerulus. The three- and four-compartment models fit the full model closely for a wide range of input levels and for both somatic and glomerular inputs. The two-compartment model gives a tolerable fit for somatic input and for low glomerular input, but deviates considerably for high glomerular input.

exhibit this behaviour, although the threshold for the transition differs slightly. Discounting the large differences which occur near this transition, the largest difference in firing rate between reduced and full models for somatic or glomerular current injection is 14% for the four compartment model and 22% for the three-compartment model (Fig. 7).

Simulation Time

The processor time taken to simulate one hundred spikes with a current injection of 0.4 μA cm^{-2} to the soma is as follows: two-compartment model 1.8 seconds; three-compartment model 2.5 s; four-compartment model 2.9 s; full model 219 s. The four-compartment model gives a 75-fold reduction in simulation time over the full model and the two-compartment model a 120-fold reduction.

DISCUSSION

The four- and three-compartment models give good qualitative and quantitative fits to the fully-detailed model. In particular they exhibit the same rather complicated calcium channel-related behaviour at high input levels as the full model, in which a calcium spike in the glomerulus causes the opening of slow potassium channels which then suppress the sodium spike at the soma. This behaviour was not a criterion for fitting—it arises naturally from the model structure.

How do the fitted parameters of the reduced models compare to those of the full model? For the full model $p = 0.056$ (lumping soma and axon areas together), $q = 0.078$, $r = 0.11$ and $s = 0.75$. These are not very dissimilar to the area ratios of the three- and four-compartment models. The axial conductances are also similar in magnitude in the full model compared to the reduced models, although the current factors α_s and α_g are greater than 1, suggesting higher input resistance for the reduced models.

How unique are the fitted parameters? The optimisation procedure we used to fit the models can only ever guarantee to find a local minimum. By restarting the search many times from different points in parameter space we are reasonably confident that the parameters we have found are close to the global minimum (combining the Simplex algorithm with simulated annealing has been shown to be the best strategy for parameter fitting for small compartmental models [17]. Our simpler strategy is less time consuming to implement and run, however). However there are certainly other minima which give good fits. For example, one

local minimum for the four-compartment model has g_{sd} effectively zero, reducing the four-compartment model to a three-compartment one with only soma, primary dendrite and glomerulus. The most tightly constrained parameters are the areas of the soma and glomerulus. The area of the secondary dendrite compartment and the g_{sd} conductance have the widest margins of error.

This investigation has emphasised the importance of using a wide input range when fitting a model. The reduced models fit the full model well within the range of firing rates 10–120 Hz. The lower end of this range corresponds to the experimental mean rate of spontaneous firing in mammals [2,6], the higher end is seen experimentally during bursts [9]. It would be possible to re-fit the model to cover a lower range if the high input regime was not of interest.

The true test of any model such as this is its behaviour in a network. The greatly improved speed (and memory requirements) of these models compared to the fully detailed model should allow network simulations with hundreds and possibly thousands of cells—still far fewer than the 60,000 or so mitral cells in the real bulb [14], but potentially allowing realistic behaviour to be simulated and a bridge built between single cell and network level properties.

The model of Bhalla and Bower is anatomically and physiologically detailed and was carefully fitted to current clamp recordings, but it is by no means the last word in mitral cell models. As new data and new models become available it will be important to adjust the reduced models to take account of these.

The next task is to produce simplified models of the other cell types in the olfactory bulb—this may be challenging for the inhibitory interneurones due to their spines—and assemble these into a network model.

ACKNOWLEDGEMENT

This work was financially supported by the Biotechnology and Biological Sciences Research Council.

REFERENCES

1. Bhalla, U. S.; Bower, J. M. Exploring parameter space in detailed single cell models: Simulations of the mitral and granule cells of the olfactory bulb. J. Neurophysiol. 69:1948–1965; 1993.
2. Bhalla, U. S.; Bower, J. M. Multiday recordings from olfactory bulb neurons in awake freely moving rats: Spatially and temporally organised variability in odorant response properties. J. Comput. Neurosci. 4:221–256; 1997.
3. Bush, P. C.; Sejnowski, T. J. Reduced compartmental models of neocortical pyramidal cells. J. Neurosci. Meth. 46:159–166; 1993.
4. Chen, W. R.; Midtgaard, J.; Shepherd, G. M. Forward and backward propagation of dendritic impulses and their synaptic control in mitral cells. Science 278:463–467; 1997.
5. Chen, W. R.; Shepherd, G. M. Membrane and synaptic properties of mitral cells in slices of rat olfactory bulb. Brain Res. 745:189–196; 1997.
6. Harrison, T. A.; Scott, J. W. Olfactory bulb responses to odor stimulation: Analysis of response pattern and intensity relationships. J. Neurophysiol. 56:1571–1589; 1986.
7. Hodgkin, A. L.; Huxley, A. F. A quantitative description of membrane current and its application to conduction and excitation in nerve. J. Physiol. 117:500–544; 1952.
8. Marder, E. From biophysics to models of network function. Annu. Rev. Neurosci. 21:25–45; 1998.
9. Motokizawa, F.; Ogawa, Y. Discharge properties of mitral/tufted cells in the olfactory bulb of cats. Brain Res. 736:285–287; 1997.
10. Nickell, W.; Shipley, M.; Behbehani, M. Orthodromic synaptic activation of rat olfactory bulb mitral cells in isolated slices. Brain Res. Bull. 39:57–62; 1996.
11. Pinsky, P. F.; Rinzel, J. Intrinsic and network rhythmogenesis in a reduced Traub model for CA3 neurons. J. Comput. Neurosci. 1:39–60; 1994.
12. Press, W. H.; Flannery, B. P.; Teukolsky, S. A.; Vetterling, W. T. Numerical recipes: The art of scientific computing. Cambridge: Cambridge University Press; 1989.
13. Rall, W. Branching dendritic trees and motoneuron membrane resistivity. Exp. Neurol. 1:491–527; 1959.
14. Royet, J.-P.; Distel, H.; Hudson, R.; Gervais, R. A re-estimation of the number of glomeruli and mitral cells in the olfactory bulb of rabbit. Brain Res. 788:35–42; 1998.
15. Stratford, K.; Mason, A.; Larkman, A.; Major, G.; Jack, J. The modelling of pyramidal neurones in the visual cortex. In: Durbin, R.; Miall, C.; Mitchison, G., eds. The computing neuron. Wokingham: Addison-Wesley; 1989:296–321.
16. Traub, R. D.; Wong, R. K. S.; Miles, R.; Michelson, H. A model of a CA3 hippocampal pyramidal neuron incorporating voltage-clamp data on intrinsic conductances. J. Neurophysiol. 66:635–650; 1991.
17. Vanier, M. C.; Bower, J. M. A comparative survey of automated parameter-searching methods for compartmental neural models. J. Comput. Neurosci. 7:149–171; 1999.